Am J Physiol Heart Circ Physiol 309: H114–H126, 2015.
First published May 1, 2015; doi:10.1152/ajpheart.00087.2015.

Cystathionine γ-lyase, a H_2S-generating enzyme, is a GPBAR1-regulated gene and contributes to vasodilation caused by secondary bile acids

Barbara Renga,[1]* Mariarosaria Bucci,[2]* Sabrina Cipriani,[1] Adriana Carino,[1] Maria Chiara Monti,[3] Angela Zampella,[2] Antonella Gargiulo,[2] Roberta d'Emmanuele di Villa Bianca,[2] Eleonora Distrutti,[4] and Stefano Fiorucci[1]

[1]*Department of Surgical and Biomedical Sciences, University of Perugia, Perugia, Italy;* [2]*Department of Pharmacy, University of Naples "Federico II," Naples, Italy;* [3]*Department of Pharmacy, University of Salerno, Salerno, Italy; and* [4]*Azienda Ospedaliera di Perugia, Perugia, Italy*

Submitted 4 February 2015; accepted in final form 23 April 2015

Renga B, Bucci M, Cipriani S, Carino A, Monti MC, Zampella A, Gargiulo A, d'Emmanuele di Villa Bianca R, Distrutti E, Fiorucci S. Cystathionine γ-lyase, a H_2S-generating enzyme, is a GPBAR1-regulated gene and contributes to vasodilation caused by secondary bile acids. *Am J Physiol Heart Circ Physiol* 309: H114–H126, 2015. First published May 1, 2015; doi:10.1152/ajpheart.00087.2015.—GPBAR1 is a bile acid-activated receptor (BAR) for secondary bile acids, lithocholic (LCA) and deoxycholic acid (DCA), expressed in the enterohepatic tissues and in the vasculature by endothelial and smooth muscle cells. Despite that bile acids cause vasodilation, it is unclear why these effects involve GPBAR1, and the vascular phenotype of GPBAR1 deficient mice remains poorly defined. Previous studies have suggested a role for nitric oxide (NO) in regulatory activity exerted by GPBAR1 in liver endothelial cells. Hydrogen sulfide (H_2S) is a vasodilatory agent generated in endothelial cells by cystathionine-γ-lyase (CSE). Here we demonstrate that GPBAR1 null mice had increased levels of primary and secondary bile acids and impaired vasoconstriction to phenylephrine. In aortic ring preparations, vasodilation caused by chenodeoxycholic acid (CDCA), a weak GPBAR1 ligand and farnesoid-x-receptor agonist (FXR), was iberiotoxin-dependent and GPBAR1-independent. In contrast, vasodilation caused by LCA was GPBAR1 dependent and abrogated by propargyl-glycine, a CSE inhibitor, and by 5β-cholanic acid, a GPBAR1 antagonist, but not by N^5-(1-iminoethyl)-L-ornithine (L-NIO), an endothelial NO synthase inhibitor, or iberiotoxin, a large-conductance calcium-activated potassium (BK_{Ca}) channels antagonist. In venular and aortic endothelial (HUVEC and HAEC) cells GPBAR1 activation increases CSE expression/activity and H_2S production. Two cAMP response element binding protein (CREB) sites (CREs) were identified in the CSE promoter. In addition, TLCA stimulates CSE phosphorylation on serine residues. In conclusion we demonstrate that GPBAR1 mediates the vasodilatory activity of LCA and regulates the expression/activity of CSE. Vasodilation caused by CDCA involves BK_{Ca} channels. The GPBAR1/CSE pathway might contribute to endothelial dysfunction and hyperdynamic circulation in liver cirrhosis.

bile acids; GPBAR1; nitric oxide; hydrogen sulfide

BILE ACIDS are amphipathic molecules synthesized in the liver from oxidation of cholesterol. Beside their role in nutrient absorption, primary bile acids, chenodeoxycholic acid (CDCA) and cholic acid (CA), and secondary bile acids, deoxycholic acid (DCA) and lithocholic acid (LCA), and their glycine and taurine conjugates, are signaling molecules exerting their role by activating a family of receptors collectively known as bile acid-activated receptors (BARs). BARs belong to the superfamilies of G protein (GP)-coupled receptors and nuclear receptors (10, 20). The best characterized BARs in these two families are the GPBAR1 (also known as TGR5) and the farnesoid-x-receptor (FXR) (10, 11). GPBAR1 is a cell surface receptor highly expressed by nonparenchymal liver cells (14), enterocytes, and endocrine intestinal cells (10, 20), and it is thought to mediate nongenomic activities of bile acids by causing the recruitment of cAMP response element binding protein (CREB) to target genes endowed with a CRE responsive element. In addition, GPBAR1 is expressed in neurons in the central and peripheral nervous system and is the putative mediator of perception of itching and pain induced by bile acids (20, 21). One specific feature of GPBAR1 is its expression by liver sinusoidal and vascular endothelial cells suggesting a role for this receptor in regulating the liver and systemic microcirculation (14, 17). In addition, GPBAR1 is expressed by smooth muscle cells and regulates smooth muscle relaxation via inhibition of Rho kinase pathway (27).

Gaseous mediators, nitric oxide (NO) and hydrogen sulfide (H_2S), are potent vasoregulatory agents located downstream to several signaling pathways in the vascular system. Previous studies have shown that BARs regulate NO and H_2S generation through an overlapping network of genomic and nongenomic effects (2, 3, 5, 19, 23, 24, 34, 37). Thus, while activation of GPBAR1 by natural and synthetic ligands modulates the expression/activity of endothelial NO synthase (eNOS) (6, 23) in liver sinusoidal and endothelial cells (5, 23), activation of FXR increases the expression/activity of cystathionine-γ-lyase (CSE), an enzyme that is central in the "trans-sulfuration pathway," which leads to generation of H_2S (29). An impairment of CSE expression/activity supports the alterations of the trans-sulfuration pathway that occurs in liver cirrhosis, leading to a combination of hyper-homocysteinemia and reduced generation of H_2S within the liver microcirculation, translating into an enhanced vasomotor tone and increased intrahepatic resistance (9, 7, 29).

Despite the fact that bile acids are vasodilatory agents that accumulate in the body of patients with liver disorders, reaching concentrations up to 50–60 μM in patients with primary biliary cirrhosis (35), whether GPBAR1 mediates vasodilation caused by individual bile acids has never been elucidated. Furthermore, since CSE-derived H_2S exerts regulatory activities in the vasculature and GPBAR1 activity is modulated by endogenous H_2S (2), we sought to investigate whether activa-

* B. Renga and M. Bucci contributed equally to this work.

Address for reprint requests and other correspondence: S. Fiorucci, Univ. of Perugia-School of Medicine, Dept. of Surgical and Biomedical Sciences-Section of Gastroenterology, Piazza L. Severi 1, Perugia 06122, Perugia, Italy (e-mail: stefano.fiorucci@unipg.it).

0363-6135/15 Copyright © 2015 the American Physiological Society

Downloaded from journals.physiology.org/journal/ajpheart (079.046.069.096) on December 2, 2020.

tion of this receptor modulates the expression/activity of CSE in the endothelium (5, 12, 15, 22, 33).

Our results demonstrate that LCA, a secondary bile acid and physiological ligand for GPBAR1, promotes a CSE-dependent vasodilation of conductance vessels (aortic rings), and that this effect is attenuated by GPBAR1$^{-/-}$ gene ablation. These data are corroborated by the demonstration that 5β-cholanic acid, a GPBAR1 antagonist, reverses vasodilation caused by LCA. Present findings provide a molecular support to the vasodilatory effects of secondary bile acids and might help to define novel therapeutic targets in patients with liver disorders and hyperdynamic circulation.

METHODS

Materials and Methods

Chemicals. Bile salts [DCA, CDCA, CA, LCA, hyocholic acid (HCA), taurolithocholic acid (TLCA), taurocholic acid (TCA), taurochenodeoxycholic acid (TCDCA), taurodeoxycholic acid (TDCA), taurohyocholic acid (THCA)], L-phenylephrine (PE), serotonin (5-HT), acetylcholine (ACh), norepinephrine (NE), the CSE inhibitor propargylglycine (PAG), the nitric oxide synthase inhibitor N^5-(1-iminoethyl)-L-ornithine (L-NIO), and the PI3 kinase inhibitor LY-294,002 were from Sigma Aldrich. 5β-Cholanic acid was synthesized by Prof. Zampella (V. Sepe, B. Renga, C. Festa, C. Finamore, D. Masullo, A. Carino, S. Fiorucci, A. Zampella, unpublished observations).

Animals. GPBAR1 null mice (generated directly into C57BL/6NCrl background), and their congenic littermates on C57BL/6NCrl mice were kindly gifted by Dr. Galya Vassileva (Schering-Plough Research Institute, Kenilworth) (36). Mice were housed under controlled temperatures (22°C) and photoperiods (12:12-h light/dark cycle), allowed unrestricted access to standard mouse chow and tap water, and allowed to acclimate to these conditions for at least 5 days before inclusion in an experiment. Authorization for animal handling was released from Ministero della Sanita, Italy, to Prof. Stefano Fiorucci, permit no. 245/2013-B.

Aortic rings preparation. Experiments on aortic rings were performed at the University of Naples. Male GPBAR1$^{+/+}$ and GPBAR1$^{-/-}$ mice of 8–10 wk of age were euthanized, and the thoracic aorta was rapidly dissected and cleaned from fat and connective tissue. Rings of 2–3 mm length were cut and placed in organ baths (2–5 ml) filled with oxygenated (95% O_2-5% CO_2) Krebs solution at 37°C and mounted to isometric force transducers (type 7006, Ugo Basile, Comerio, Italy) and connected to a Graphtec line recorder (WR 3310). The composition of the Krebs solution was as follows (mol/l): 0.118 NaCl, 0.0047 KCl, 0.0012 $MgCl_2$, 0.0012 KH_2PO_4, 0.0025 $CaCl_2$, 0.025 $NaHCO_3$, and 0.010 glucose. Rings were initially stretched until a resting tension of 0.5 g was reached and allowed to equilibrate for at least 30 min during which tension was adjusted, when necessary, to 0.5 g, and bathing solution was periodically changed. In a preliminary study, a resting tension of 0.5 g was found to develop the optimal tension to stimulation with contracting agents. In each experiment aortic rings were first challenged with PE (10^{-6} mol/l) until the responses were reproducible. To verify the integrity of the endothelium, ACh cumulative concentration-response curve (from 10^{-8} to 10^{-5} M) was performed on PE contracted rings. Vessels that relaxed <85% were discarded.

In a separate set of experiments, aortic rings harvested from wild-type mice were denuded from endothelium by gently rubbing the internal surface of the vascular lumen. Rings were then challenged with PE (1 μM) and once plateau was reached a cumulative concentration-response curve to CDCA, CA, and LCA (from 10^{-8} to 10^{-4} M) was performed.

To investigate the role of GPBAR1 in LCA-induced vasodilatation, aortic ring were incubated with 5β-cholanic acid, a selective GPBAR-1 antagonist. Following PE-induced contraction, the cumulative concentration-response curve to LCA (from 10^{-8} to 10^{-4} M) was examined.

Plasma bile acid determination. The stock solutions of the individual tauroconjugated and unconjugated bile acids were prepared separately in methanol at a concentration of 1 mg/ml. All stock solutions were stored at −20°C. Calibration standards were prepared by combining appropriate volumes of each bile acid stock solution and methanol. The calibration range was from 10 nmol/l to 100 mmol/l of each bile acid in the final solution. Serum sample aliquots of 100 μl were deproteinized with 1 ml cold acetonitrile (ACN) with 5% NH_4OH, vortexing for 1 min. After centrifugation at 16,000 *g* for 10 min, the clear supernatant was transferred to a new vial, snap-frozen, and lyophilized. The sample was then redissolved in methanol and water [2:1 volume for volume (vol/vol)] for tauroconjugated bile acid determination and in methanol-ammonium acetate 10 mmol/l with 0.005% formic acid (3:2 vol/vol) for unconjugated bile acid determination. A bile acid extraction yield of 95% was measured with the addition of bile acid standard in plasma samples before and after the deproteinization procedure (25).

Liquid chromatography and mass spectrometry. For liquid chromatography-tandem mass spectrometry (MS/MS) analysis, chromatographic separation was carried out on the LTQ XL high-performance liquid chromatography mass spectrometry system (ThermoScientific) equipped with the Accelera 600 Pump and Accelera AutoSampler system. The mixture was separated on a Jupiter 5 μm C18 Å column (150 × 2.00 mm) (Phenomenex). Tauroconjugated bile acids were separated at a flow rate of 200 μl/min using a methanol-aqueous ammonium acetate (NH_4OAc) gradient. Mobile phase A was 5% methanol in water containing 2 mM ammonium acetate at pH 7; mobile phase B was methanol, containing ammonium acetate at 2 mM. The gradient started at 30% B and increased to 100% B in 20 min, kept at 100% B for 5 min, then decreased to 30% B in 1 min and kept at 30% B for 10 min. ESI was performed in negative ion mode; the ion source temperature was set at 280°C. The tune page parameters were automatically optimized injecting taurocholic acid at 1 μM as standard. The MS/MS detection was operated in MRM mode using a collision energy of 20 (arbitrary units); the observed transitions were tauro-β-muricholic acid (tbMCA) at 13.5 min MRM of 514.28 Th → 514.28 Th, tHCA at 15.6 min MRM of 498.29 Th → 498.29 Th, tCA at 16.6 min MRM of 514.28 Th → 514.28 Th, tCDCA at 18.5 min MRM of 498.29 Th → 498.29 Th, tDCA at 18.9 min MRM of 498.29 Th → 498.29 Th, and tLCA at 22.35 min MRM of 482.29 Th → 482.29 Th. Unconjugated bile acids were separated at a flow rate of 200 μl/min using 10 mM ammonium acetate in water at 0.005% formic acid as the mobile phase A, and 10 mM ammonium acetate in methanol at 0.005% formic acid as mobile phase B. The gradient program started at 60% B and increased to 95% B in 25 min, kept at 95% B for 9 min, then decreased to 60% B in 1 min and kept at 60% B for 10 min. ESI was performed in negative ion mode; the ion source temperature was set at 280°C. The tune page parameters were automatically optimized injecting CA at 1 μM as standard. The MS/MS detection was operated in MRM mode using a collision energy of 15 (arbitrary units). The observed transitions were HCA at 8.9 min MRM of 391.29 Th → 391.29 Th, CA at 10.2 min MRM of 407.28 Th → 407.28 Th, CDCA at 13.8 min MRM of 391.29 Th → 391.29 Th, DCA at 14.4 min MRM of 391.29 Th → 391.29 Th, and LCA at 17.5 min MRM of 375.28 Th → 375.28 Th.

Cell culture, RNA extraction, and real-time PCR. Human aortic endothelial cells (HAEC) and human umbilical endothelial cells (HUVEC) were cultured in Medium 200 (Life Technologies) containing LSGS (Life Technologies) and antibiotics.

To investigate the mRNA expression of GPBAR1, CBS, CSE and eNOS, HAEC and HUVEC cells serum starved O/N were stimulated with 10 μM TLCA for 18 h. To investigate the role of GPBAR1 in the

Downloaded from journals.physiology.org/journal/ajpheart (079.046.069.096) on December 2, 2020.

regulation of CSE mRNA expression, HUVEC cells serum starved O/N were stimulated for 18 h with 10 μM TLCA or with the combination of TLCA plus 5β-cholanic acid (50 μM).

Total RNA was isolated from endothelial cells using the TRIzol reagent according to the manufacturer's specifications (Life Technologies). One microgram of RNA was purified from genomic DNA by DNase-I treatment (Life Technologies) and reverse-transcribed using random hexamer primers with Superscript-II (Life Technologies) in a 20-μl reaction volume. Ten nanograms cDNA was amplified in a 20 μl solution containing 200 nM of each primer and 10 μl of KAPA SYBR FAST Universal qPCR Kit (KAPA BIOSYSTEMS). All reactions were performed in triplicate, and the thermal cycling conditions were as follows: 3 min at 95°C, followed by 40 cycles of 95°C for 15 s, 56°C for 20 s and 72°C for 30 s. The relative mRNA expression was calculated accordingly with the C_t method. PCR primers were designed using the software PRIMER3 (http://frodo.wi.mit.edu/primer3/) using published sequence data obtained from the NCBI database. Forward and reverse primer sequences were hGAPDH, gaaggtgaaggtcggagt and catgggtggaatcatattggaa; hCSE, cactgtccaccacgttcaag and gtggctgctaaacctgaagc; hCBS, tcgtgatgccagagaagatg and ttggggatttcgttcttcag; hTGR5, cactgttgtccctcctctcc and acactgctttggctgcttg; and heNOS, agtgaaggcgacaatcctgtat and agggacaccacgtcatactcat.

Western blotting. To investigate protein expression of GPBAR1 and CSE, HAEC and HUVEC cells serum starved O/N were stimulated with 10 μM TLCA for 18 h. Total lysates were prepared by solubilization of endothelial cells in NuPage sample buffer (Life Technologies) containing Sample Reducing Agent (Invitrogen) and separated by PAGE. The proteins were then transferred to nitrocellulose membranes (Bio-Rad) and probed with primary antibodies CSE (Santa Cruz), GPBAR1/TGR5 (Abcam), tubulin (Sigma), phospho-Akt (Santa Cruz), Akt (Santa Cruz), and phospho-serine (Abcam). Nitrocellulose membranes were first probed with a phospho-serine antibody and then stripped and reprobed with the CSE antibody. Similarly, nitrocellulose membranes were first probed with the phospho-Akt antibody, stripped, and then reincubated with the Akt antibody. The anti-immunoglobulin G horseradish peroxidase conjugate (Bio-Rad) was used as the secondary antibody, and specific protein bands were visualized using Super Signal West Dura (Pierce), following the manufacturer's suggested protocol (30).

CSE promoter analysis, plasmid construction, and luciferase assay. Human, murine, and rat proximal promoter regions of CSE gene were analyzed with the on-line software TFsearch (http://www.cbrc.jp/research/db/TFSEARCH.html) for searching of putative CREB consensus sequences. For luciferase assay, five tandem repeats of the putative CRE1 and CRE2 responsive sequences were cloned *Kpn*I-*Xho*I into the pGL4 luciferase reporter vector. HEK-293T cells were transfected with 200 ng of pGL4$(CRE1)_{5X}$ or pGL4$(CRE2)_{5X}$ or with pGL4.29 (a reporter vector containing a canonical cAMP response element), with 100 ng of pCMVSPORT6-human GPBAR1 and with 100 ng of pGL4.70 (a vector encoding the human Renilla gene). Forty-eight hours posttransfection, cells were stimulated 18 h with a dose response of TLCA (1, 10, and 50 μM). Control cultures received vehicle (0.1% DMSO) alone. Cells were lysed in 100 μl diluted reporter lysis buffer (Promega), and 10 μl of cellular lysate was assayed for luciferase activity using the Glomax 20/20 luminometer (Promega, Milan, Italy). Luciferase activities were normalized for transfection efficiencies by dividing the relative luciferase units (RLU) by Renilla activities (RRU).

CSE protein analysis. To identify potential phosphorylation sites on human, mouse, and rat CSE (CTH) proteins we used a PhosphoSite Plus (http://www.phosphosite.org) software, an open interactive resource for investigating experimentally posttranslational modifications. To predict which kinases may target particular Ser, Thr, or Tyr residues we used the on-line software Scansite3 (scansite3.mit.edu).

Immunoprecipitation. Overnight serum starved HUVECs were stimulated with TLCA (10 μM) for 0, 5, 15, 30, and 60 min. After stimulation, cells were washed with cold PBS and lysed in 500 μl E1A lysis buffer containing protease and phosphatase inhibitors. Lysates were sonicated and clarified by centrifugation at 13,000 *g* for 10 min, and the protein concentrations were determined by Bradford assay. Five-hundred micrograms total proteins were precleared on a rotating wheel for 1 h at 4°C using protein A Sepharose beads (Amersham Biosciences) and 1 μg of irrelevant antibody of the same species and isotype as CSE. Immunoprecipitation was performed overnight at 4°C with 1 μg CSE antibody (Santa Cruz) or anti-IgG as a negative control antibody in the presence of 40 μl of protein A Sepharose (Amersham Biosciences). The resultant immunoprecipitates were washed five times with 1 ml of E1A lysis buffer and then used for Western blotting.

Chromatin immunoprecipitation. Serum starved HUVEC cells (10×10^6) were stimulated 18 h with 10 μM TLCA or received the vehicle alone (1% DMSO). Chromatin was immunoprecipitated with an anti-phosphoCREB antibody (Santa Cruz) or with an anti-IgG as negative control. Detailed methods for ChIP protocol and Real-Time data analysis have been previously described (30). The sequences of primers used for the amplification of the human CRE1 and CRE2 promoter sequences were CRE1, ctggtctcgaactcttgacttcag and gctaacgcctattaatcccagcac; CRE2, gtggtctgtttacagttacccggt and tgccatgctggctcctgaga.

Electrophoretic mobility shift assay. Nuclear extracts from serum starved HUVEC cells left untreated or stimulated 18 h with TLCA (10 μM) were prepared using the NE-PER kit (Pierce). Nuclear extracts (10 μg) were incubated for 20 min at room temperature with 20 fmol of biotin-labeled CRE1 probe (GCCT**TGACTTCA**TGCA) or with biotin-labeled CRE2 probe (GCCT**TGAGGTCA**TGCA), prior to electrophoresis. For competition experiments, 250-fold excess of unlabeled probes or anti-phosphoCREB antibody (Santa Cruz) were incubated for 20 min with nuclear extracts from stimulated cells before addition of the biotin-labeled probes.

CSE activity. CSE activity was performed as previously described (29). HUVEC and HAEC cells serum starved O/N were stimulated with 10 μM TLCA for 18 h. To investigate on the role of PI3K/Akt in the regulation of CSE activity HUVEC cells serum starved O/N were stimulated for 18 h with 10 μM TLCA or with the combination of TLCA plus LY-294,002 (10 μM). To investigate the role of GPBAR1 in the regulation of CSE activity, HUVEC cells serum starved O/N were stimulated for 18 h with 10 μM TLCA or with the combination of TLCA plus 5β-cholanic acid (50 μM).

Statistical analysis. All values are means ± SE of number (*n*) of observations per group. Comparisons were made by one-way ANOVA with post hoc Tukey's test. Comparison of two groups was made by the Student's *t*-test for unpaired data when appropriate.

RESULTS

Vasoconstriction and Vasodilation in GPBAR1$^{-/-}$ Mice

We have first characterized the liver and vascular phenotype of GPBAR1$^{-/-}$ mice compared with their congenic littermates. GPBAR1 null mice had normal serum levels of AST but slight increase of bilirubin (Fig. 1, *A* and *B*). The mean arterial pressure (MAP) was similar to that of congenic mice (Fig. 1*C*). In contrast, quantitative analysis of serum bile acids revealed that GPBAR1$^{-/-}$ mice had higher concentrations of circulating bile acids, reaching a value of ~200 μM [Fig. 1*D*, $P < 0.05$ vs. wild-type (WT) animals]. Analysis of individual bile acid species demonstrates that concentrations of nonconjugated (HCA, CA, CDCA, DCA, and LCA) and taurine-conjugated (TβMCA, THCA, TCA, TCDCA, TDCA, and TLCA) bile acids were higher in mice harboring a disrupted GPBAR1 (Fig. 1, *E* and *F*, $P < 0.05$ vs. WT animals). When these changes were expressed as a

Downloaded from journals.physiology.org/journal/ajpheart (079.046.069.096) on December 2, 2020.

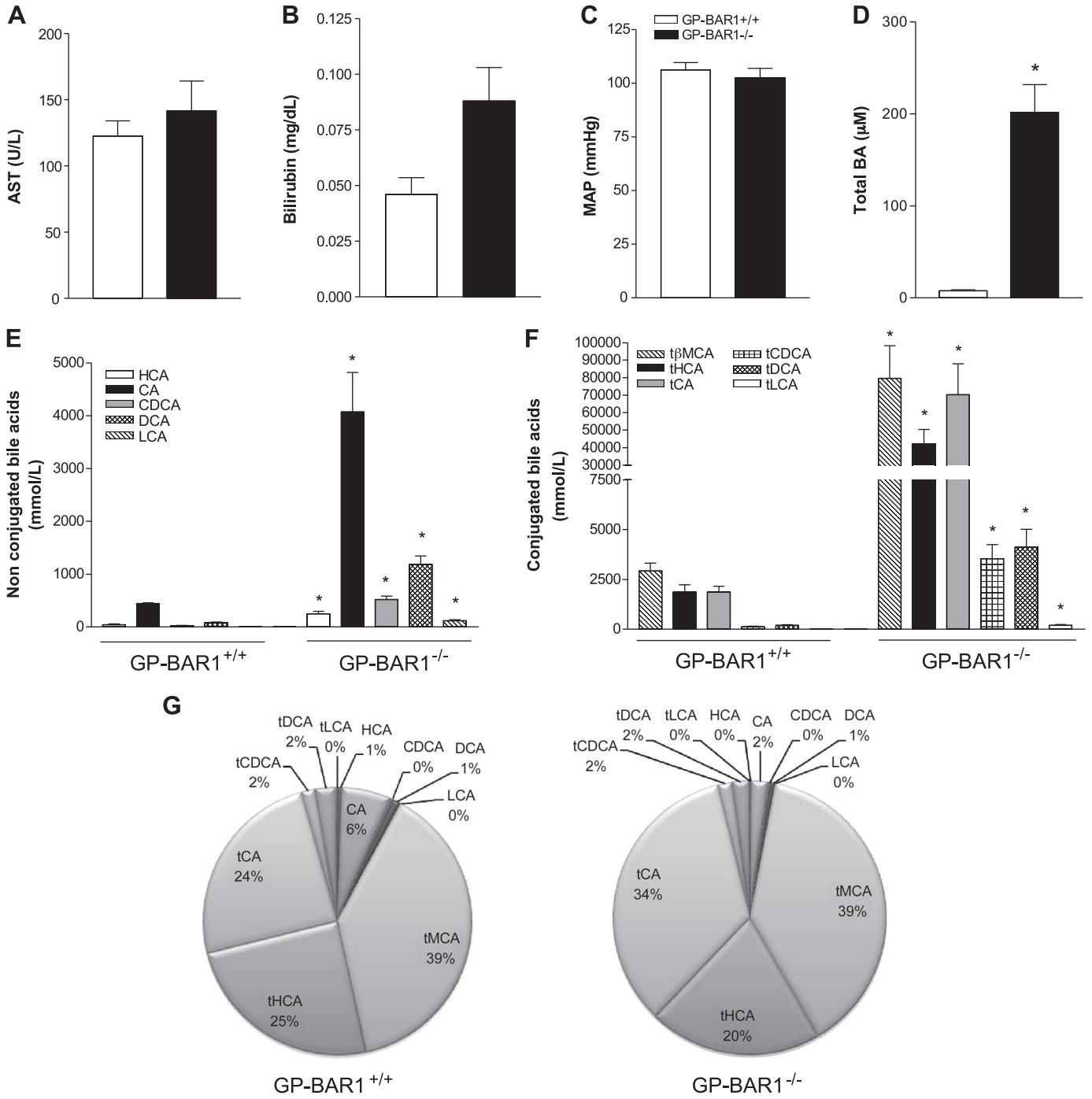

Fig. 1. GPBAR1 gene ablation results in normal mean arterial pressure (MAP) but altered bile acid (BA) metabolism. *A–C*: serum levels of AST, total bilirubin, and MAP in GPBAR1$^{+/+}$, and GPBAR1$^{-/-}$ mice. *D*: total plasma bile acids concentrations. *E* and *F*: plasmatic concentrations of nonconjugated (*E*) and conjugated (*F*) bile acids in GPBAR1$^{+/+}$ and GPBAR1$^{-/-}$ mice. *G*: qualitative analysis of serum bile acid composition in GPBAR1$^{+/+}$ and GPBAR1$^{-/-}$ mice. Data are means ± SE of 8 mice per group. CA, cholic acid; LCA, lithocholic acid; DCA, deoxycholic acid; CDCA, chenodeoxycholic acid; HCA, hyocholic acid; tCA, taurocholic acid; tLCA, taurolithocholic acid; tDCA, taurodeoxycholic acid; tCDCA, taurochenodeoxycholic acid; tHCA, taurohyocholic acid; tβMCA, tauro-β-muricholic acid. GPBAR1, G protein-coupled bile acid receptor 1. *$P < 0.05$ vs. GPBAR1$^{+/+}$ mice.

percentage of total bile acids (Fig. 1*G*), GPBAR1 null mice had a robust increase of TCA (from 24% to 34%), as well as a decrease of CA (from 6 to 2%).

Vasodilation Induced by LCA is Impaired in GPBAR1$^{-/-}$ Mice

GPBAR1 gene ablation results in multiple functional alterations of conductance vessels. Indeed, as illustrated in Fig. 2, *A–C*, aortic rings prepared from GPBAR1$^{-/-}$ mice had a slight but significant impairment of the contractile response to PE but not to 5-HT (Fig. 2, *A* and *B*, $P < 0.05$ vs. WT animals). Furthermore, vasodilation caused by acetylcholine was slightly enhanced in animals harboring a disrupted GPBAR1 (Fig. 2*C*, $P < 0.05$ vs. WT animals).

Downloaded from journals.physiology.org/journal/ajpheart (079.046.069.096) on December 2, 2020.

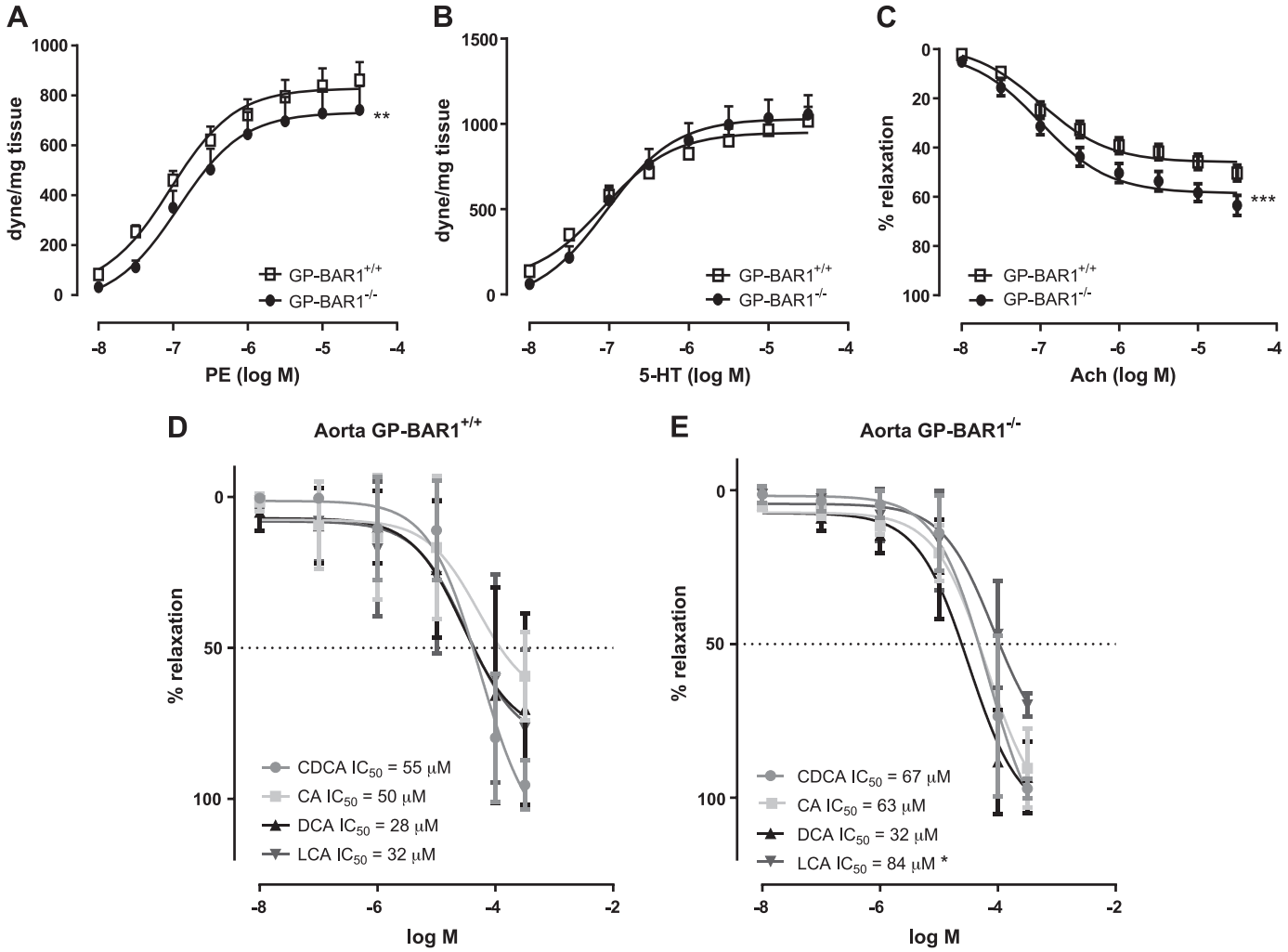

Fig. 2. Aortic rings isolated from GPBAR1 deficient mice show altered vasodilation and vasocontraction. *A*: contractile response to phenylephrine (PE) in aortic rings from both GPBAR1$^{+/+}$ and GPBAR1$^{-/-}$ mice. *B*: contractile response to 5-HT in aortic rings from GPBAR1$^{+/+}$ and GPBAR1$^{-/-}$ mice. *C*: vasorelaxant effect of ACh in aortic rings from GPBAR1$^{+/+}$ and GPBAR1$^{-/-}$ mice. *D* and *E*: vasorelaxant effect of CDCA, CA, DCA, and LCA on aortic rings isolated from GPBAR1$^{+/+}$ (*E*) and GPBAR1$^{-/-}$ (*F*) mice. Data are means ± SE of 8 mice per group. $^{**}P < 0.05$ vs. GPBAR1$^{+/+}$ mice; $^{***}P < 0.01$ vs. GPBAR1$^{+/+}$ mice.

To investigate whether GPBAR1 mediates vasodilation caused by bile acids, we then assessed the vasomotor activity of individual bile acids using aortic rings prepared from wild-type and GPBAR1$^{-/-}$ mice. As shown in Fig. 2, *D* and *E*, exposure of aortic rings to CDCA, CA, and DCA resulted in a robust vasodilation that was fully conserved in GPBAR1$^{-/-}$ mice. However, aortic rings from GPBAR1$^{-/-}$ mice displayed an attenuated vasodilatory response to LCA. Thus the EC_{50} of LCA-induced vasodilation of PE-contracted rings increased ~3-fold from 34 to 84 μM (Fig. 2, *D* and *E*, $P < 0.05$ vs. WT animals). Because the vasodilation caused by LCA appears to be partially dependent on a conserved GPBAR1 signaling, we then investigated downstream signals involved in this effect. As shown in Fig. 3, *A* and *B*, incubation of aortic rings with propargylglycine (PAG), a nonselective CSE inhibitor, abrogated the vasodilatory effect of LCA in GPBAR1$^{+/+}$ mice but failed to reverse vasodilation caused by this agent in GPBAR1 null animals (Fig. 3, *A* and *B*, $P < 0.05$ vs. WT animals). Of interest, PAG had no effect on vasodilation induced by CDCA (Fig. 3*C*).

In contrast to PAG, L-NIO, a nonselective eNOS inhibitor, had no effect on vasodilation induced by LCA in wild-type mice (Fig. 4*A*). Because NO is known to mediate the endothelium-dependent vasodilation, we have further examined whether vasodilation caused by LCA was endothelium dependent by challenging endothelium-deprived aortic ring with primary and secondary bile acids. We have demonstrated the efficacy of endothelium deprivation procedure by generating a dose-response curve to acetylcholine (Fig. 4*B*). Results shown in Fig. 4, *C–E*, demonstrate that vasodilation caused by LCA was maintained in endothelium-deprived aortic rings, thereby confirming results obtained with L-NIO ($n = 4$) and indicating that vasodilatory action of bile acids is largely due to a direct interaction with smooth muscle cells.

Vasodilation caused by LCA was also resistant to iberiotoxin (100 nM) both in wild-type and GPBAR1$^{-/-}$ mice, while vasodilation caused by CDCA was reduced by a coincubation with the calcium-activated large-conductance K channels (BK_{Ca}) inhibitor (Fig. 5, *A* and *B*).

Downloaded from journals.physiology.org/journal/ajpheart (079.046.069.096) on December 2, 2020.

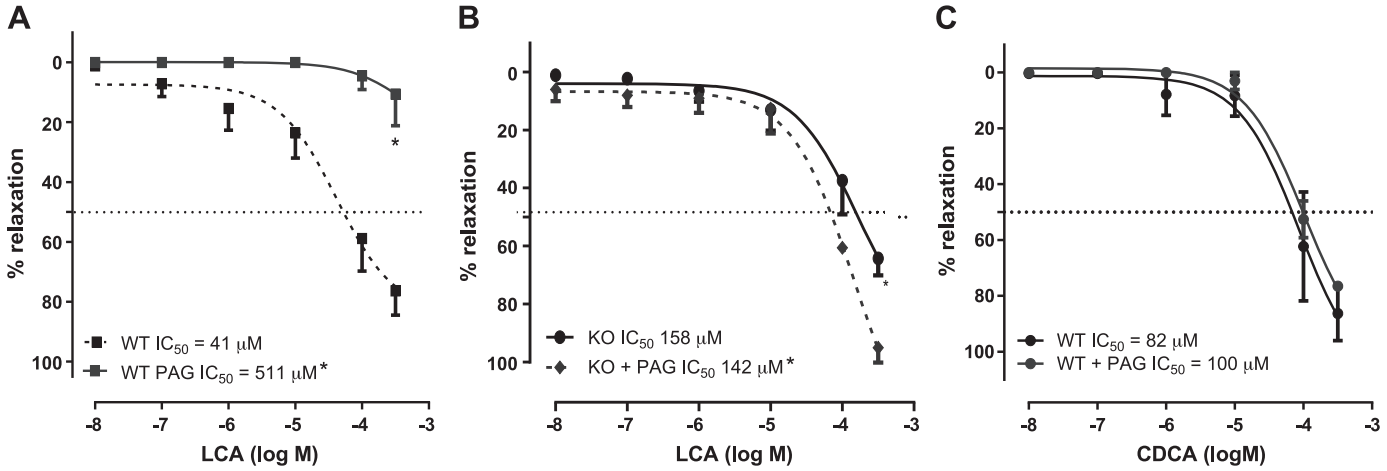

Fig. 3. CSE inhibition attenuate vasodilation caused by GPBAR1 agonism. Cystathionine-γ-lyase (CSE) inhibitor propargylglycine (PAG) abrogates vasorelaxant effect of LCA on aortic rings from GPBAR1$^{+/+}$ mice (*A*) but not from GPBAR1$^{-/-}$ [knockout (KO)] mice (*B*). *C*: PAG did not modulate the vasorelaxant effect of CDCA on aortic rings from wild-type mice. Data are means ± SE of 8 mice per group. *$P < 0.05$ vs. GPBAR1$^{+/+}$ mice.

GPBAR1 Regulates CSE Expression/Activity in Human Endothelial Cells

Because these data demonstrate that vasodilation caused by LCA is eNOS independent but is reversed by PAG, a CSE inhibitor, in a GPBAR1-dependent manner, we sought to define the molecular mechanisms involved in this effect using human arterial and venular endothelial cells. First of all we have examined whether GPBAR1 deficiency results in dysregulated expression of CSE and eNOS in the aortas. However, as predicted by the fact that these mice had normal MAP, the

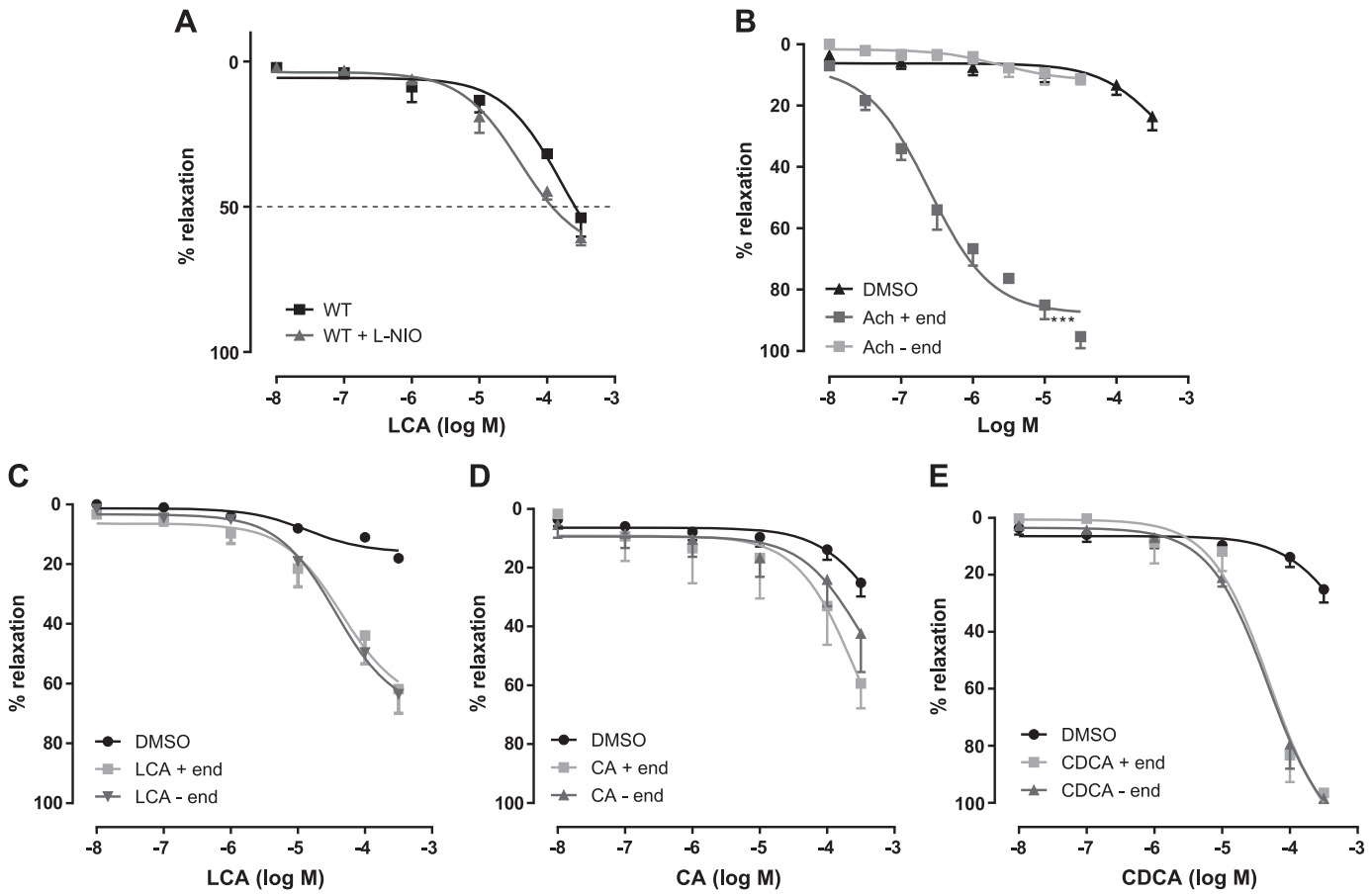

Fig. 4. Vasodilation caused by LCA is endothelium independent. *A*: N^5-(1-iminoethyl)-L-ornithine (L-NIO), a nonspecific inhibitor of endothelial nitric oxide synthase (eNOS), fails to attenuate vasodilation caused by LCA. Data are means ± SE of 8 mice per group. *B*: vasorelaxant effect of ACh in aortic rings left intact (+end) or denuded from endothelium (−end). *C–E*: aortic rings denuded from endothelium were challenged with PE (1 μM) and then treated with various concentrations (from 10^{-8} to 3×10^{-4} M) of LCA (*B*), CA (*C*), and CDCA (*D*). Data are means ± SE of 8 mice per group. ***$P < 0.01$ vs. DMSO.

Downloaded from journals.physiology.org/journal/ajpheart (079.046.069.096) on December 2, 2020.

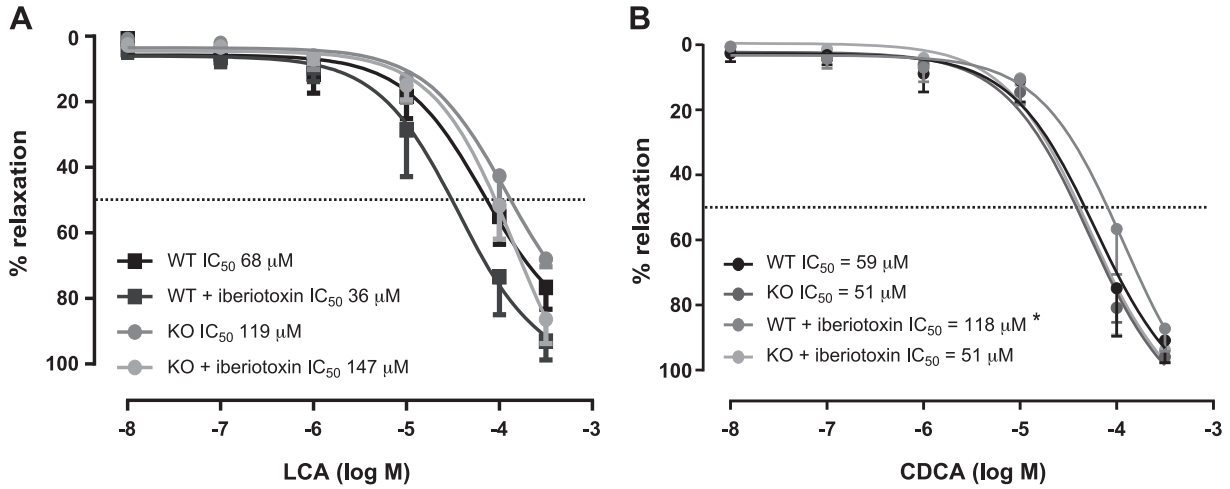

Fig. 5. Vasodilation caused by GPBAR1 is iberiotoxin resistant. *A*: iberiotoxin (a specific inhibitor of calcium-activated potassium channels) does not block vasorelaxant effect of LCA in aortic rings from GPBAR1$^{+/+}$ and GPBAR1$^{-/-}$ mice. *B*: iberiotoxin reduces vasorelaxant effect of CDCA on aortic rings from GPBAR1$^{+/+}$ mice while it does not change CDCA mediated vasodilation on aortic rings from GPBAR1$^{-/-}$ mice. Data are means ± SE of 8 mice per group. *$P < 0.05$ vs. GPBAR1$^{+/+}$ mice.

expression of CSE and eNOS in the aortas along with circulating levels of H_2S and nitrite/nitrate were similar to that of their congenic littermates (data not shown). Because GPBAR1$^{-/-}$ mice had elevated levels of primary and secondary bile acids, that activate multiple BARs, making it difficult to dissect individual signals in these animals, we have further examined the role of GPBAR1 signaling using endothelial cells. Expression of GPBAR1 mRNA was detected in HAEC cells, and the stimulation of these cells with TLCA (10 μM) induced the expression of CSE, mRNA, and protein, while no significant changes in the relative expression of CBS, eNOS, and GPBAR1 gene expression were detected (Fig. 6*A*, $P <$ 0.05 vs. untreated cells). However, exposure to TLCA resulted in a time-dependent phosphorylation of eNOS (data not shown). Consistent with these results, CSE activity increased in HAEC treated with TLCA (Fig. 6*B*, $P < 0.05$ vs. untreated cells). All together these results demonstrated that GPBAR1 activation by TLCA in HAEC cells results in a positive regulation of CSE expression/activity. These results were confirmed in human umbilical endothelial cells (HUVEC). In these cells, TLCA effectively induced both CSE mRNA and protein expression and increased CSE enzyme activity (Fig. 6, *C* and *D*).

GPBAR1 Promotes the Recruitment of CREB to the CSE Promoter

Because GPBAR1 signals by recruiting the transcription factor CREB to CREB responsive elements (CRE) in the promoter of target genes, we have searched for putative CREs in the promoter of CSE. The analysis of the 5′-flanking region of human, mouse, and rat CSE gene revealed the presence of two conserved CRE, we named CRE1 and CRE2. In the human CSE promoter the CRE1 is located at −1,502 base pairs (bp) with respect to the transcriptional starting site ATG, while the CRE2 is located at −467 bp (Fig. 7*A*). To explore the functionality of these putative CREs in regulating the CSE expression, five copies of the CRE1 and CRE2 were cloned in a pGL4 vector and transfected into HEK293T cells also transiently transfected with GPBAR1. The luciferase reporter assay results shown in Fig. 7, *B–D*, demonstrated that the activation of these two CREs by TLCA was concentration-dependent and required 50 and 10 μmol/l TLCA, respectively, for CRE1 and CRE2. To verify the hypothesis that CREB binds the putative CREs in the CSE promoter, we then performed an EMSA experiment using biotin-labeled probes against CRE1 and CRE2. These probes were incubated with nuclear extracts from HUVEC cells not treated or stimulated with TLCA. As shown in Fig. 7, *E* and *F*, a slight supershift was observed when CRE1 and CRE2 probes were incubated with nuclear extracts from naive cells while the exposure to TLCA strongly induced these interactions (Fig. 7*E*, *lanes 2* and *3*; Fig. 7*F*, *lanes 2* and *3*). We confirmed the specificity of these interactions by adding 250-fold excess of unlabeled CRE1 and CRE2 probes or 1 μg anti-phospho-CREB antibody (Fig. 7*E*, *lanes 4* and *5*; Fig. 7*F*, *lanes 4* and *5*). Furthermore, results from CHIP experiment shown in Fig. 7, *G* and *H*, confirmed that CREB binds the CSE promoter in basal conditions on both CRE1 and CRE2 and that these interactions were strongly enhanced in cells exposed to TLCA. Thus the functionality of the two CREs sites was confirmed in the context of intact chromatin structures.

GPBAR1 Promotes Protein Phosphorylation and Increases CSE Activity

Because effects exerted by LCA in aortic rings bath are more compatible with rapid activation of CSE rather than gene regulation, we have examined whether LCA exerts non-genomic effects on CSE. One such regulatory pathway, similarly to eNOS, could be protein phosphorylation. Theoretical prediction of phosphorylation sites on CSE protein sequence was performed using PhosphoSite Plus and Scansite3 software. As shown in Fig. 8*A*, PhosphoSite Plus predicted a total of 10 conserved phosphorylation sites in human, mouse, and rat CSE protein corresponding to Ser8, Ala51, Tyr60, Tyr114, Ile140, Thr158, Thr160, Thr163, Ser282, and Ser377 residues of human CSE protein. To understand which kinases might phosphorylate these sites we have applied to human CSE the Scansite algorithm, which uses position-specific scoring matrices (PSSMs) for 32 kinases, including a set of PSSMs for several mitotic kinases. The analysis of phosphorylation sites

Downloaded from journals.physiology.org/journal/ajpheart (079.046.069.096) on December 2, 2020.

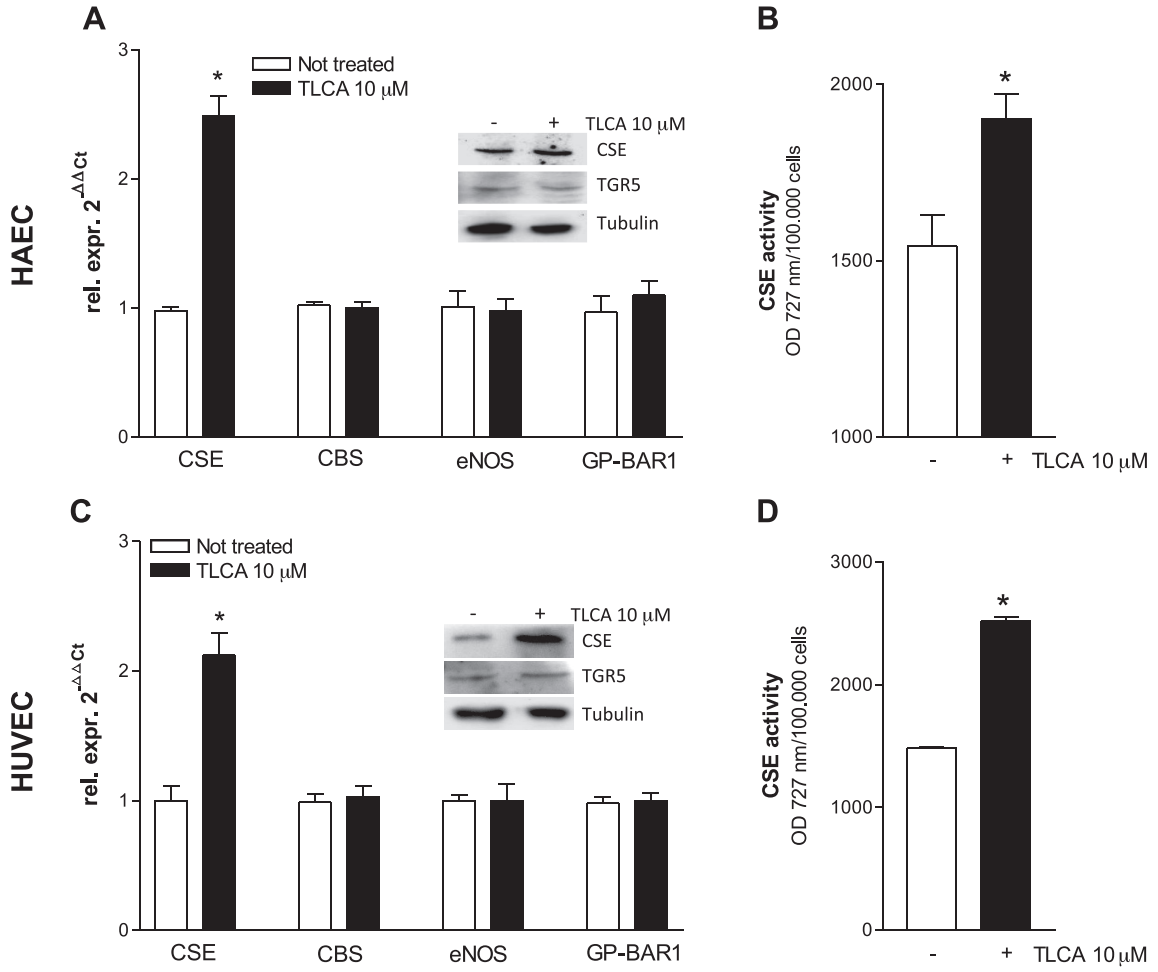

Fig. 6. GPBAR1 activation regulates CSE expression in endothelial cells. *A*: relative mRNA expression of CSE, cystathionine β-synthase (CBS), eNOS, and GPBAR1 (TGR5) on HAEC cells left untreated or administered 18 h with TLCA (10 μM). Western blot analysis of CSE and TGR5 on HAEC cells. Data are means ± SE of 4 experiments. *$P < 0.05$ vs. not treated cells. *B*: CSE activity on HAEC stimulated 48 h with TLCA (10 μM). *$P < 0.05$ vs. not treated cells. *C*: relative mRNA expression of CSE, CBS, eNOS, and GPBAR1 (TGR5) on HUVEC cells left untreated or administered 18 h with TLCA (10 μM). Western blot analysis of CSE and TGR5 on HUVEC cells. Data are means ± SE of 4 experiments. *$P < 0.05$ vs. not treated cells. *D*: CSE activity on HUVEC cells stimulated 48 h with TLCA (10 μM). *$P < 0.05$ vs. not treated cells.

predicted by Scansite at high stringency is shown in Table 1. Of note, comparison of the Scansite motifs matched to the sites within our dataset with all phosphorylation sites present in the PhosphoSitePlus database, revealing that Ser377 may be a substrate for AKT1 and cAMP dependent protein kinase PKACG, two downstream signals triggered by GPBAR1. To validate our bioinformatic analysis we next performed immunoprepitation experiments. We first subjected HUVEC cells to time course treatment with TLCA to evaluate the phosphorylation status of Akt. As shown in Fig. 8*B* we found that exposure to TLCA increases the level of phosphorylated Akt1 protein within 5 min of treatment, and this activation was maintained until 60 min (Fig. 8*B*). The effect of GPBAR1 activation on phosphorylation status of CSE protein was quantified by immunoprecipitation with an anti-CSE antibody followed by Western blot analysis using an anti-phosphoserine, anti-Akt1, and anti-phospho-Akt1 antibodies. Results from immunoprecipitation experiments demonstrated the existence of a protein complex between the proteins CSE and Akt1 which is clearly assembled already in basal conditions (Fig. 8*C*). Of interest, the interaction between CSE and Akt1 (both phosphorylated or total) in HUVEC increased after 5 min stimulation with TLCA (Fig. 8*C*). Moreover, 30 min treatment with TLCA increased the phosphorylation of CSE on serine residues without affecting total CSE protein levels (Fig. 8*C*). Finally, to further demonstrate the role of PI3K/Akt in mediating CSE phosphorylation, HUVEC were coincubated with a PI3K kinase inhibitor, LY-294,002. Results from enzyme activity assay demonstrated that pretreating HUVEC with LY-294,002 resulted in a significant reduction of TLCA-mediated activation of CSE activity (Fig. 8*D*).

GPBAR1 Antagonism by DFN406 Locks Vasodilatory Effect of LCA

To further tie activation of GPBAR1 to CSE activity in HUVEC cells, we then carried out experiments using a GPBAR1 antagonist. As shown in Fig. 9*A*, incubation of aortic rings with 5β-cholanic acid, a GPBAR1 antagonist, significantly reduced LCA-induced vasodilatation, suggesting that GPBAR1 activation contributes to the vasodilatory action of LCA observed in this study. In addition, results from both

Downloaded from journals.physiology.org/journal/ajpheart (079.046.069.096) on December 2, 2020.

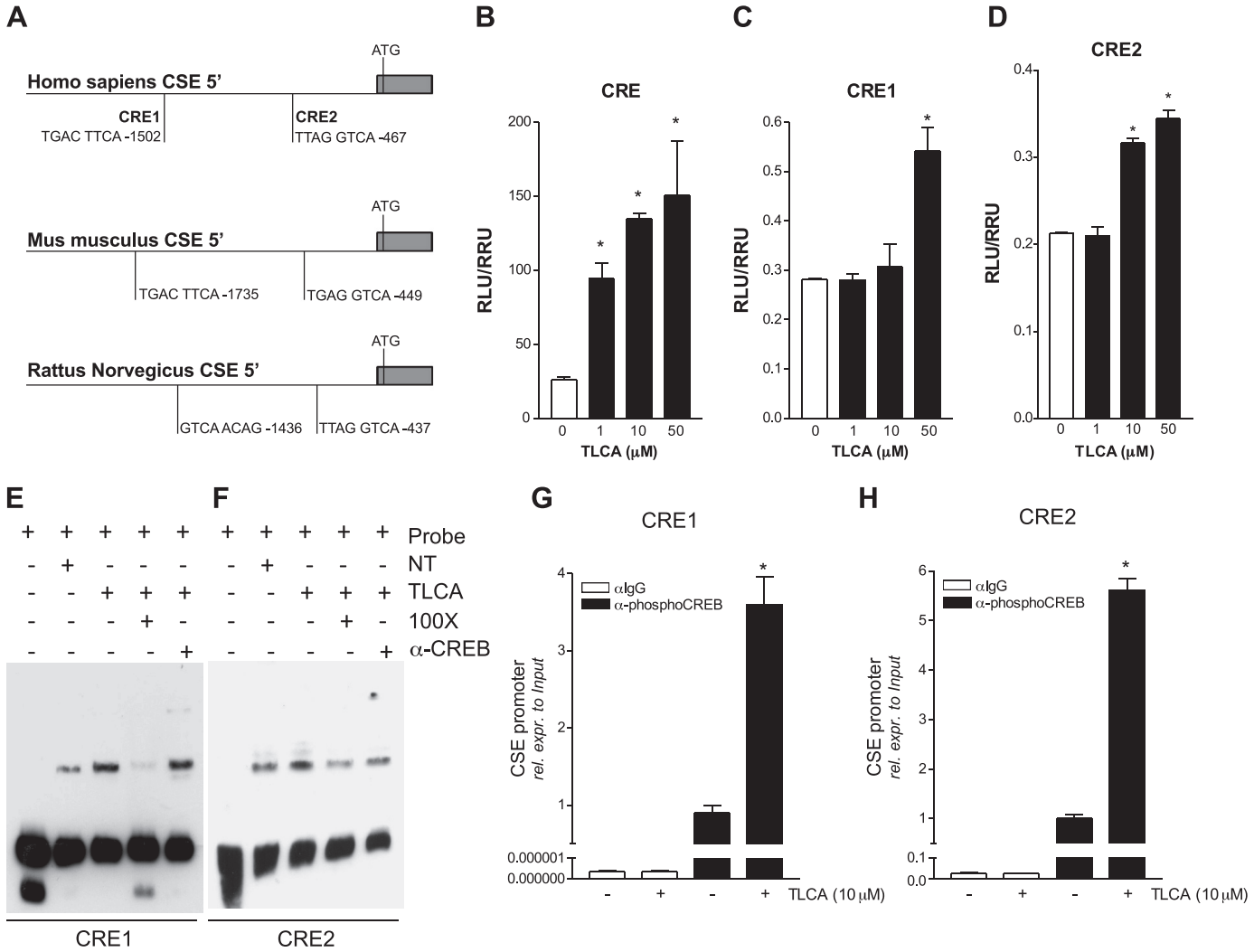

Fig. 7. Genomic regulation of CSE by TLCA is mediated by cAMP responsive elements (CRE). *A*: analysis of human, mouse, and rat CSE promoter showing two conserved putative CRE sequences named CRE1 and CRE2. Promoter analysis was performed with the on-line software TFsearch. *B–D*: three copies of the human CRE1 (or CRE2) were cloned into the luciferase reporter vector pGL4. HUVEC cells were transiently transfected with pCMVSPORT-hTGR5 and $pGL4(CRE1)_{5X}$ (*C*) or with pCMVSPORT-hTGR5 and $pGL4(CRE2)_{5X}$ (*D*), and 48 h posttransfection cells were stimulated 18 h with TLCA (10 μM). Cellular extracts were subsequently assayed for luciferase activity. As positive control HUVEC cells were transiently transfected with pCMVSPORT-hTGR5 and with a reporter vector containing a canonical cAMP response element (*B*). Data are the means ± SE of 3 experiments carried out in triplicate. $*P < 0.05$ vs. not treated cells. *E* and *F*: electrophoretic mobility shift assay (EMSA). Nuclear extracts from HUVEC cells left not treated (NT) or stimulated with TLCA were incubated in the presence of a CRE1 (*E*) or a CRE2 (*F*) biotin-labeled probe. Competition experiments were performed with a 100-fold excess of unlabeled oligo or with 1 μg CREB antibody. The image shown is one of three showing the same pattern. *G* and *H*: chromatin immunoprecipitation (ChIP). ChIP assay carried out in HUVEC left untreated or primed with TLCA as described in *Materials and Methods*. RT-PCR was performed with specific primers flanking the responsive element CRE1 (*G*) or CRE2 (*H*) on human CSE promoter. Values are normalized relative to input DNA concentration and are expressed relative to those of not treated cells immunoprecipitated with an anti-IgG antibody condition, set as 1. Analysis was carried out in triplicate and the experiment was repeated twice. $*P <$ 0.05 vs. not treated cells immunoprecipitated with an anti-phospho-CREB antibody.

RT-PCR and enzyme activity assay demonstrated that the pretreatment of HUVEC with DFN406 attenuates regulation of CSE (mRNA expression and enzyme activity) caused by TLCA (Fig. 9, *B* and *C*).

DISCUSSION

Patients with liver cirrhosis and portal hypertension develop hypotension and attenuated vascular tone, which has been associated to a NO-dependent impairment of peripheral vascular responses (4, 31), leading to a hyperdynamic circulation. Despite that this syndrome might have several mechanistic explanations, it is well understood that, as liver disease progresses toward cirrhosis, the bile acid pool shifts from the enterohepatic to the systemic circulation (13, 26). This increased concentration of bile acids might be a causative factor in the pathogenesis of the hyperdynamic state occurring in the end stage of liver disorders (4).

By using mice that were deficient for GPBAR1 (36), we have now shown that vasodilation caused by primary and secondary bile acids occurs through a GPBAR1-dependent mechanisms. Additionally, we have provided evidence that GPBAR1 activation regulates the expression/activity of CSE, an enzyme that is critical for the generation of H_2S, and that CSE inhibition caused by PAG reverses the vasodilatory effect

Downloaded from journals.physiology.org/journal/ajpheart (079.046.069.096) on December 2, 2020.

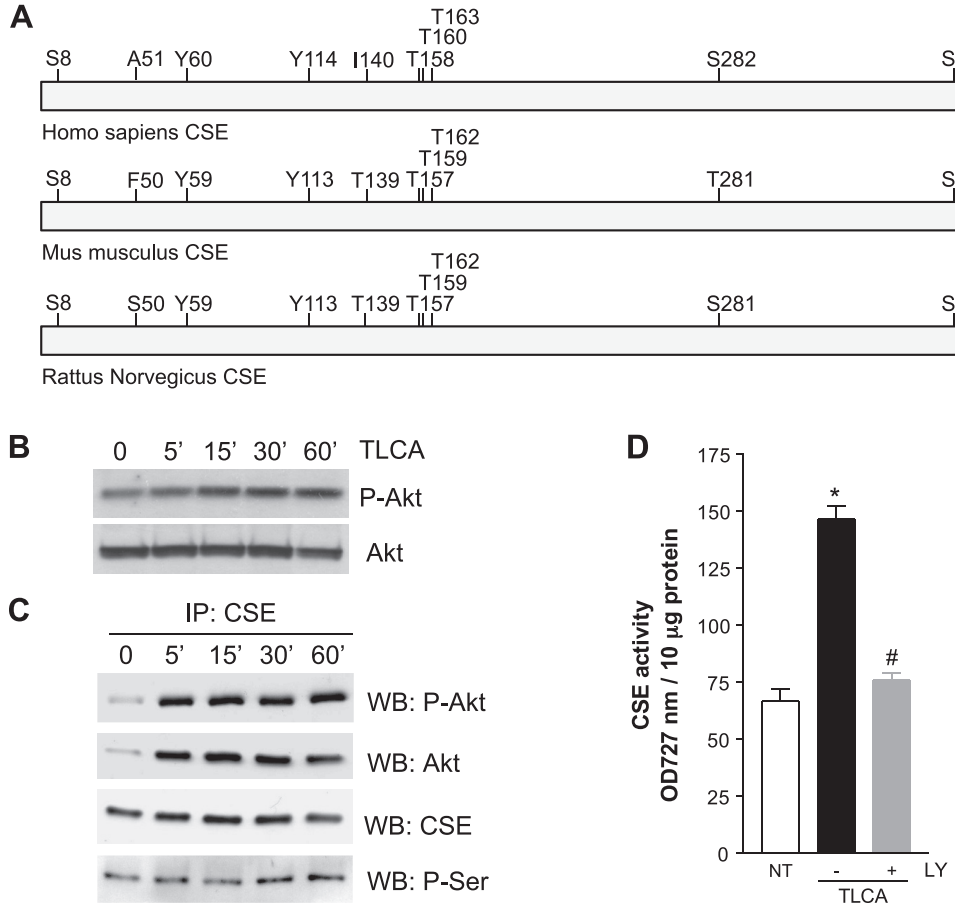

Fig. 8. Nongenomic regulation of CSE by TLCA is mediated by serine phosphorylation. *A*: overview of phosphorylation sites identified in human, mouse, and rat CSE protein using the PhosphoSite plus software. *B*: representative Western blot of Akt1 and phospho-Akt1 proteins in HUVEC exposed to TLCA (10 μM) for 0, 5, 15, 30, and 60 min. The blot shown is one of three showing the same pattern. *C*: effect of TLCA on phosphorylation of CSE on serine residues. Serine phosphorylation of CSE was assessed by immunoprecipitation of CSE followed by Western blot determination of phosphoserine and phospho-Akt1 content in HUVEC exposed to TLCA (10 μM) for 0, 5, 15, 30, and 60 min. The blot shown is one of three showing the same pattern. *D*: effect of PI3K inhibitor LY-294,002 (LY) on CSE enzyme activity in HUVEC coadministered with TLCA. $*P < 0.05$ vs. not treated (NT) cells; $\#P < 0.05$ vs. TLCA-treated cells.

exerted by LCA (and TLCA) in wild-type mice, but not in GPBAR1$^{-/-}$ mice.

GPBAR1 is expressed in the vascular system. However, GPBAR1$^{-/-}$ mice do not develop overt alterations in their vascular phenotype and have a normal MAP despite the fact that circulating bile acids were significantly higher than that of their congenic littermates. Furthermore, results from ex vivo experiments carried out using aortic rings demonstrate that vasodilation caused by primary bile acids is maintained in GPBAR1$^{-/-}$ mice. Only vasodilation caused by LCA, a potent GPBAR1 ligand, was significantly reduced by the ablation of the receptor as demonstrated by a 3-fold increase in EC_{50} required by LCA to elicit a full vasodilatory response. Because vasodilation caused by primary bile acids, CDCA and CA, was maintained in GPBAR1$^{-/-}$ mice it appears that GPBAR1-independent mechanisms mediate the activity of these bile acids. Importantly, CDCA and CA are poor ligands for GPBAR1. Indeed, the EC_{50} required for GPBAR1 activation in CHO cells transfected with GPBAR1 (TGR5) by TLCA, LCA, DCA, CDCA, and CA was reported to be 0.33, 0.53, 1.01, 4.43, and 7.72 μm, respectively (13). Further, in addition to GPBAR1, CDCA and CA activate a number of receptors/channels including FXR and BK_{Ca} (8), type 3 of muscarinic receptor (16), and K_{ATP} channels via a cAMP-protein kinase A-dependent mechanism (18). Activation of these receptors and channels might explain the fact that vasodilation caused by CDCA and CA is maintained in GPBAR1$^{-/-}$ mice. Vice versa, because LCA and DCA also activate these receptors, although with a different rank of potencies, it appears difficult to dissect individual pathways in vivo, when multiple bile acid species are present.

Because vasodilation caused by LCA was attenuated by GPBAR1 gene ablation we have focused our attention on the mechanisms that support this effect. Data shown in Fig. 3 demonstrate that while vasodilation caused in wild-type mice by LCA is blunted by exposure to PAG, an inhibitor of CSE activity (1), this inhibitory effect was lost in GPBAR1$^{-/-}$ mice, thereby establishing that, at least in naive mice, vasodilation caused by LCA implies a GPBAR1/CSE-mediated pathway.

An important finding we made in this study was that vasodilation caused by bile acids was maintained in aortic rings denuded from endothelium. This observation along with the fact that L-NIO, a selective inhibitor of eNOS, had no detectable effect on vasodilation caused by LCA in wild-type mice, despite that LCA induces in vitro phosphorylation of eNOS

Downloaded from journals.physiology.org/journal/ajpheart (079.046.069.096) on December 2, 2020.

Table 1. *Motif scanning of phosphorylation sites in the CSE protein sequence*

Position	Kinase (Gene ID)	Score	Description
S8	CSNK1G2	0.523	Casein kinase 1, gamma2
S8	AURKB	0.878	Aurora kinase B
S8	PRKDC	0.707	Protein Kinase, DNA-activated, catalytic peptide
S8	ATM	0.691	ATM serine/threonine kinase
A51			
Y60			
Y114	LCK	0.493	LCK proto-oncogene, Src family tyrosine kinase
Y114	SRC	0.594	SRC proto-oncogene, nonreceptor tyrosine kinase
I140			
T158	CDK1	0.605	Cyclin-dependent kinase 1
T158	CDC2	0.711	Cyclin-dependent kinase A-1
T158	CDK5	0.682	Cyclin-dependent kinase 5
T158	MAPK3	0.649	Mitogen-activated protein kinase 3
T160			
T163	PRKDC	0.553	Protein kinase, DNA activated, catalytic polypeptide
S282			
S377	AKT1	0.752	v-akt thymoma viral oncogene homolog 1
S377	AURKA	0.538	Aurora kinase A
S377	AURKB	0.435	Aurora kinase B
S377	CAMK2G	0.642	Calcium/calmodulin-dependent protein kinase II gamma
S377	PKCE	0.562	Protein kinase C, epsilon
S377	PKACG	0.523	Protein kinase, cAMP-dependent, catalytic, gamma

CSE, cystathionine-γ-lyase.

(data not shown), support the notion that GPBAR1-mediated vasodilatory effect are only in part due to the activation of endothelium. Indeed, Rajagopal et al. (27) have shown that GPBAR1 is expressed by and regulates smooth muscle cell relaxation via both Epac- and PKA-mediated inhibition of the RhoA/Rho kinase pathway.

Furthermore, vasodilation caused by LCA was iberiotoxin-resistant in both wild-type and GPBAR1$^{-/-}$ mice, thus indicating that LCA induces a vasodilation through a BK_{Ca}-independent and GPBAR1/CSE-mediated mechanism in wild-type mice. In contrast, vasodilation caused by CDCA was iberiotoxin sensitive, thereby suggesting that this bile acid activates BK_{Ca} channels. Our observation is consistent with the findings that in dogs, vasodilation caused by synthetic GPBAR1 ligands is only partially sensitive to iberiotoxin (12). The fact that L-NIO failed to attenuate vasodilation caused by LCA, despite that it causes the phosphorylation of eNOS, is also consistent with the observation that L-NAME does not attenuate vasodilation caused by synthetic GPBAR1 ligands in dogs (12).

CREB is a cyclic AMP response element (CRE)-binding protein activated following GPBAR1 ligation by bile acids (32). In the present study we have identified two CRE sequences in the promoter of CSE (28). The CRE elements are conserved across species, and their functionality was confirmed by a variety of molecular approaches in HUVEC. Thus, by luciferase reporter gene assays, we have observed that GPBAR1 activation by TLCA increases the transcriptional activity on human CSE promoter, while chromatin immunoprecipitation experiments have provided robust evidence that GPBAR1 activation recruits CREB in its active form to the human region of CSE promoter that contains the two CREB binding sites. Finally, results of EMSA experiments confirmed that the transcription factor CREB binds to both proximal and distal CRE sequences and that the incubation of nuclear extracts with a specific antibody directed against the active form of CREB abrogates the binding of nuclear extracts to the CRE1 or CRE2 biotin-labeled probes. Taken together these results provide a molecular explanation to the potent inhibitory effect exerted by PAG on vasodilation caused by LCA.

GPBAR1 signals through the activation of cAMP/PKA and PI3K/Akt pathways (17, 27). Analysis of putative phosphorylation sites of CSE performed with PhosphoSite plus software and Scansite algorithm revealed that this enzyme might be

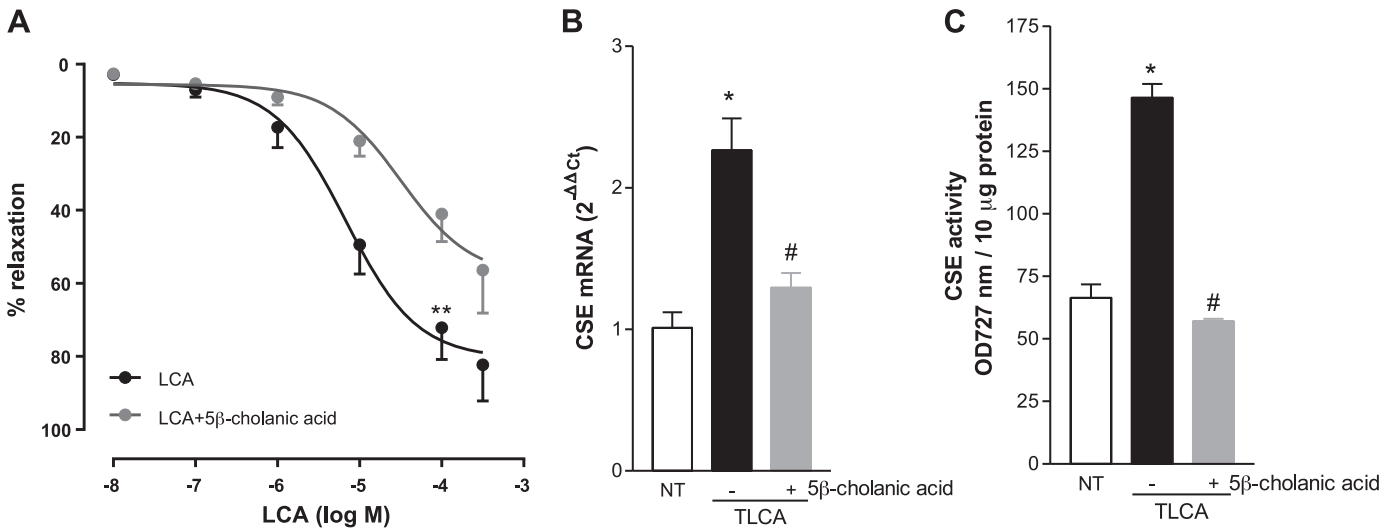

Fig. 9. GPBAR1 antagonism by 5β-cholanic acid reverses vasodilation and attenuates CSE expression and activity induced by TLCA. *A*: effect of GPBAR1 antagonist 5β-cholanic acid on vasodilatory activity of LCA. *B* and *C*: effect of GPBAR1 antagonist 5β-cholanic acid on mRNA expression (*B*) and enzyme activity (*C*) of CSE in HUVEC left untreated or administered with TLCA. $^{**}P < 0.05$ vs. LCA + 5β-cholanic acid; $^{*}P < 0.05$ vs. not treated cells; $\#P < 0.05$ vs. LCA-treated cells.

Downloaded from journals.physiology.org/journal/ajpheart (079.046.069.096) on December 2, 2020.

phosphorylated by Akt and cAMP-dependent PKA on serine resides, in particular Ser377. Western blotting and immunoprecipitate experiments have confirmed that TLCA increases Akt phosphorylation and results in a significant increase in CSE phosphorylation on serine residues. To support this observation, experiments conducted in HUVEC demonstrated that CSE activity was abrogated in cells coadministered with TLCA and LY-294,002, a PI3K inhibitor. The role of GPBAR1 in regulation of CSE was further demonstrated by the finding that GPBAR1 antagonism by 5β-cholanic acid abrogates vasodilation-reversed CSE activation caused by TLCA.

The fact that GPBAR1 gene deletion had no effect on aortic expression of CSE and eNOS mRNAs (data not shown) should be interpreted taking into account that GPBAR1 gene ablation alters bile acid metabolism, resulting in elevated levels of primary and secondary bile acids, which activate multiple receptors, a conundrum that is inherent to the model and to the pleiotropic function of each bile acid.

The present findings have clinical relevance since patients with liver disorders are characterized by altered systemic circulation. This vasodilatory syndrome results in an enhanced risk of fatal complications, and its pathogenesis is controversial. We have now provided evidence that circulating bile acids acting on endothelial and muscular receptors might play a mechanistic role. The fact that a GPBAR1 antagonist blunts the vasodilatory effect caused by TLCA paves the way for development of novel therapies.

In conclusion, we have demonstrated that primary and secondary bile acids are vasodilatory agents and that vasodilation induced by LCA is GPBAR1 dependent and involves the regulation of CSE expression/activity in endothelial and muscular cells. Despite that primary and secondary bile acids activate a variety of receptors and mediators, the present findings might help to interpret the systemic hemodynamic changes in patients with liver cirrhosis.

DISCLOSURES

No conflicts of interest, financial or otherwise, are declared by the author(s).

AUTHOR CONTRIBUTIONS

Author contributions: B.R., M.B., S.C., A.C., M.C.M., A.Z., A.G., and R.d.d.V.B. performed experiments; B.R., M.B., S.C., A.C., M.C.M., A.Z., A.G., R.d.d.V.B., and S.F. analyzed data; B.R. and S.F. interpreted results of experiments; B.R., E.D., and S.F. prepared figures; B.R., E.D., and S.F. drafted manuscript; S.F. conception and design of research; S.F. edited and revised manuscript; S.F. approved final version of manuscript.

REFERENCES

1. **Asimakopoulou A, Panopoulos P, Chasapis CT, Coletta C, Zhou Z, Cirino G, Giannis A, Szabo C, Spyroulias GA, Papapetropoulos A.** Selectivity of commonly used pharmacological inhibitors for cystathionine β synthase (CBS) and cystathionine γ lyase (CSE). *Br J Pharmacol* 169: 922–932, 2013.
2. **Bala V, Rajagopal S, Kumar DP, Nalli AD, Mahavadi S, Sanyal AJ, Grider JR, Murthy KS.** Release of GLP-1 and PYY in response to the activation of G protein-coupled bile acid receptor TGR5 is mediated by Epac/PLC-ε pathway and modulated by endogenous H_2S. *Front Physiol* 2014 Nov 3; 5:420. doi:10.3389/fphys.2014.00420. eCollection 2014.
3. **Bishop-Bailey D, Walsh DT, Warner TD.** Expression and activation of the farnesoid X receptor in the vasculature. *Proc Natl Acad Sci USA* 101: 3668–3673, 2004.
4. **Bolognesi M, Di Pascoli M, Verardo A, Gatta A.** Splanchnic vasodilation and hyperdynamic circulatory syndrome in cirrhosis. *World J Gastroenterol* 20: 2555–2563, 2014.
5. **Bomzon A, Ljubuncic P.** Bile acids as endogenous vasodilators? *Biochem Pharmacol* 49: 581–589, 1995.
6. **Bucci M, Papapetropoulos A, Vellecco V, Zhou Z, Zaid A, Giannogonas P, Cantalupo A, Dhayade S, Karalis KP, Wang R, Feil R, Cirino G.** cGMP-dependent protein kinase contributes to hydrogen sulfide-stimulated vasorelaxation. *PLoS One* 7: e53319, 2012.
7. **Distrutti E, Mencarelli A, Santucci L, Renga B, Orlandi S, Donini A, Shah V, Fiorucci S.** The methionine connection: homocysteine and hydrogen sulfide exert opposite effects on hepatic microcirculation in rats. *Hepatology* 47: 659–667, 2008.
8. **Dopico AM, Walsh JV Jr, Singer JJ.** Natural bile acids and synthetic analogues modulate large conductance Ca^{2+}-activated K^+ (BK_{Ca}) channel activity in smooth muscle cells. *J Gen Physiol* 119: 251–273, 2002.
9. **Fiorucci S, Antonelli E, Mencarelli A, Orlandi S, Renga B, Rizzo G, Distrutti E, Shah V, Morelli A.** The third gas: H_2S regulates perfusion pressure in both the isolated and perfused normal rat liver and in cirrhosis. *Hepatology* 42: 539–548, 2005.
10. **Fiorucci S, Mencarelli A, Palladino G, Cipriani S.** Bile-acid-activated receptors: targeting TGR5 and farnesoid-X-receptor in lipid and glucose disorders. *Trends Pharmacol Sci* 30: 570–580, 2009.
11. **Fiorucci S, Distrutti E, Ricci P, Giuliano V, Donini A, Baldelli F.** Targeting FXR in cholestasis: hype or hope. *Expert Opin Ther Targets* 18: 1449–1459, 2014.
12. **Fryer RM, Ng KJ, Nodop Mazurek SG, Patnaude L, Skow DJ, Muthukumarana A, Gilpin KE, Dinallo RM, Kuzmich D, Lord J, Sanyal S, Yu H, Harcken C, Cerny MA, Hickey ER, Modis LK.** G protein-coupled bile acid receptor 1 stimulation mediates arterial vasodilation through a K(Ca)1.1 [BK(Ca)]-dependent mechanism. *J Pharmacol Exp Ther* 348: 421–431, 2014.
13. **Kawamata Y, Fujii R, Hosoya M, Harada M, Yoshida H, Miwa M, Fukusumi S, Habata Y, Itoh T, Shintani Y, Hinuma S, Fujisawa Y, Fujino M.** A G protein-coupled receptor responsive to bile acids. *J Biol Chem* 278: 9435–9440, 2003.
14. **Keitel V, Reinehr R, Gatsios P, Rupprecht C, Görg B, Selbach O, Häussinger D, Kubitz R.** The G-protein coupled bile salt receptor TGR5 is expressed in liver sinusoidal endothelial cells. *Hepatology* 45: 695–704, 2007.
15. **Khurana S, Yamada M, Wess J, Kennedy RH, Raufman JP.** Deoxycholyltaurine-induced vasodilation of rodent aorta is nitric oxide- and muscarinic M(3) receptor-dependent. *Eur J Pharmacol* 517: 103–110, 2005.
16. **Khurana S, Raufman JP, Pallone TL.** Bile acids regulate cardiovascular function. *Clin Transl Sci* 4: 210–218, 2011.
17. **Kida T, Tsubosaka Y, Hori M, Ozaki H, Murata T.** Bile acid receptor TGR5 agonism induces NO production and reduces monocyte adhesion in vascular endothelial cells. *Arterioscler Thromb Vasc Biol* 33: 1663–1669, 2013.
18. **Lavoie B, Balemba OB, Godfrey C, Watson CA, Vassileva G, Corvera CU, Nelson MT, Mawe GM.** Hydrophobic bile salts inhibit gallbladder smooth muscle function via stimulation of GPBAR1 receptors and activation of K_{ATP} channels. *J Physiol* 588: 3295–3305, 2010.
19. **Li J, Wilson A, Kuruba R, Zhang Q, Gao X, He F, Zhang LM, Pitt BR, Xie W, Li S.** FXR-mediated regulation of eNOS expression in vascular endothelial cells. *Cardiovasc Res* 77: 169–177, 2008.
20. **Lieu T, Jayaweera G, Bunnett NW.** GPBA: a GPCR for bile acids and an emerging therapeutic target for disorders of digestion and sensation. *Br J Pharmacol* 17: 1156–1166, 2014.
21. **Lieu T, Jayaweera G, Zhao P, Poole DP, Jensen D, Grace M, McIntyre P, Bron R, Wilson YM, Krappitz M, Haerteis S, Korbmacher C, Steinhoff MS, Nassini R, Materazzi S, Geppetti P, Corvera CU, Bunnett NW.** The bile acid receptor TGR5 activates the TRPA1 channel to induce itch in mice. *Gastroenterology* S0016–S5085: 1081–1086, 2014.
22. **Ljubuncic P, Said O, Ehrlich Y, Meddings JB, Shaffer EA, Bomzon A.** On the in vitro vasoactivity of bile acids. *Br J Pharmacol* 131: 387–398, 2000.
23. **Marazioti A, Bucci M, Coletta C, Vellecco V, Baskaran P, Szabó C, Cirino G, Marques AR, Guerreiro B, Gonçalves AM, Seixas JD, Beuve A, Romão CC, Papapetropoulos A.** Inhibition of nitric oxide-stimulated vasorelaxation by carbon monoxide-releasing molecules. *Arterioscler Thromb Vasc Biol* 31: 2570–2576, 2011.

Downloaded from journals.physiology.org/journal/ajpheart (079.046.069.096) on December 2, 2020.

24. **Mencarelli A, Renga B, Distrutti E, Fiorucci S.** Antiatherosclerotic effect of farnesoid X receptor. *Am J Physiol Heart Circ Physiol* 296: H272–H281, 2009.
25. **Mencarelli A, Renga B, D'Amore C, Santorelli C, Graziosi L, Bruno A, Monti MC, Distrutti E, Cipriani S, Donini A, Fiorucci S.** Dissociation of intestinal and hepatic activities of FXR and LXRα supports metabolic effects of terminal ileum interposition in rodents. *Diabetes* 62: 3384–3393, 2013.
26. **Pirotte J.** Modification of serum bile acid levels and clearance in liver disorders. *Acta Gastroenterol Belg* 51: 503–508, 1988.
27. **Rajagopal S, Kumar DP, Mahavadi S, Bhattacharya S, Zhou R, Corvera CU, Bunnett NW, Grider JR, Murthy KS.** Activation of G protein-coupled bile acid receptor, TGR5, induces smooth muscle relaxation via both Epac- and PKA-mediated inhibition of RhoA/Rho kinase pathway. *Am J Physiol Gastrointest Liver Physiol* 304: G527–G535, 2013.
28. **Renga B.** Hydrogen sulfide generation in mammals: the molecular biology of cystathionine-β-synthase (CBS) and cystathionine-γ-lyase (CSE). *Inflamm Allergy Drug Targets* 10: 85–91, 2011.
29. **Renga B, Mencarelli A, Migliorati M, Distrutti E, Fiorucci S.** Bile-acid-activated farnesoid X receptor regulates hydrogen sulfide production and hepatic microcirculation. *World J Gastroenterol* 15: 2097–2108, 2009.
30. **Renga B, Mencarelli A, D'Amore C, Cipriani S, Baldelli F, Zampella A, Distrutti E, Fiorucci S.** Glucocorticoid receptor mediates the gluconeogenic activity of the farnesoid X receptor in the fasting condition. *FASEB J* 26: 3021–3031, 2012.
31. **Ryan J, Sudhir K, Jennings G, Esler M, Dudley F.** Impaired reactivity of the peripheral vasculature to pressor agents in alcoholic cirrhosis. *Gastroenterology* 105: 1167–1172, 1993.
32. **Shaywitz AJ, Greenberg ME.** CREB: a stimulus-induced transcription factor activated by a diverse array of extracellular signals. *Annu Rev Biochem* 68: 821–861, 1999.
33. **Sheikh Abdul Kadir SH, Miragoli M, Abu-Hayyeh S, Moshkov AV, Xie Q, Keitel V, Nikolaev VO, Williamson C, Gorelik J.** Bile acid-induced arrhythmia is mediated by muscarinic M2 receptors in neonatal rat cardiomyocytes. *PLoS One* 5: e9689, 2010.
34. **Sinal CJ, Tohkin M, Miyata M, Ward JM, Lambert G, Gonzalez FJ.** Targeted disruption of the nuclear receptor FXR/BAR impairs bile acid and lipid homeostasis. *Cell* 102: 731–744, 2000.
35. **Trottier J, Białek A, Caron P, Straka RJ, Heathcote J, Milkiewicz P, Barbier O.** Metabolomic profiling of 17 bile acids in serum from patients with primary biliary cirrhosis and primary sclerosing cholangitis: a pilot study. *Dig Liver Dis* 44: 303–310, 2012.
36. **Vassileva G, Golovko A, Markowitz L, Abbondanzo SJ, Zeng M, Yang S, Hoos L, Tetzloff G, Levitan D, Murgolo NJ, Keane K, Davis HR Jr, Hedrick J, Gustafson EL.** Targeted deletion of GPBAR1 protects mice from cholesterol gallstone formation. *Biochem J* 398: 423–430, 2006.
37. **Zhang R, Ran HH, Zhang YX, Liu P, Lu CY, Xu Q, Huang Y.** Farnesoid X receptor regulates vascular reactivity through nitric oxide mechanism. *J Physiol Pharmacol* 63: 367–372, 2012.

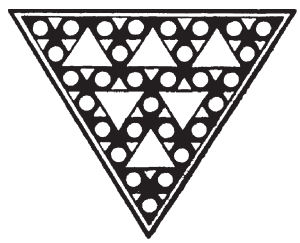

Downloaded from journals.physiology.org/journal/ajpheart (079.046.069.096) on December 2, 2020.